Available online at www.sciencedirect.com
SCIENCE DIRECT®
Physica A 341 (2004) 495–525
PHYSICA A
www.elsevier.com/locate/physa

Small-scale turbulence in the plankton: low-order deterministic chaos or high-order stochasticity?

Laurent Seuront[a,b,*]

[a] School of Biological Sciences, Flinders University, GPO Box 2100, Adelaide 5001, South Australia
[b] Ecosystem Complexity Research Group, Station Marine de Wimereux, CNRS UMR 8013 ELICO, Université des Sciences et Technologies de Lille, BP 80, F-62930 Wimereux, France

Received 27 January 2004

Abstract

Almost all regions of the oceans are heavily influenced by the effects of physical processes such as turbulence which in turn influence the distribution and ecology of organisms that occupy these regions. There is a real need for additional focus placed on the precise knowledge of both physical and biological processes which is often difficult using basic time series analysis. In that way, we applied nonlinear analysis techniques to high frequency time series of temperature, salinity and phytoplankton concentrations recorded in different hydrodynamical regimes related to tidal forcing in a tidally mixed coastal ecosystem. Techniques devoted to the identification of low-order deterministic chaos cannot find evidence of chaos. While a lower dimensionality was identified in low hydrodynamic conditions, the results rather suggest stochastic time series with many degrees of freedom: no obvious attractor in phase space trajectory, LLE indistinguishable from zero, absence of convergence of the correlation integral. We then applied to these data specific multifractal analysis techniques and showed that these time series clearly exhibit high-order stochasticity. In addition, the stochastic structure of purely passive scalars (i.e., temperature and salinity) remained invariant, while the one of phytoplankton biomass must be regarded as highly structured in time by both hydrodynamic and advective processes.

PACS: 87.10.+e; 47.53.+n

Keywords: Turbulence; Phytoplankton; Patchiness; Scaling; Multiscaling; Chaos; Determinism; Stochasticity

* Ecosystem Complexity Research Group, Station Marine de Wimereux, CNRS UMR 8013 ELICO, Université des Sciences et Technologies de Lille, BP 80, F-62930 Wimereux, France. Fax: +33+3-21992901.
E-mail addresses: laurent.seuront@univ-lille1.fr, laurent.seuront@flinders.edu.au (L. Seuront).

0378-4371/$ - see front matter
doi:10.1016/j.physa.2004.04.128

1. Introduction

Since the seminal studies of chaos in discrete time models in population ecology [1–3], the issue of chaotic dynamics in ecological systems has been widely controversial [4–6]. Chaos in ecology has nevertheless been the subject of an increasing amount of literature. In theoretical ecology, there are many examples of temporal population models which exhibit chaos. The interaction of three variables in a predator-prey-nutrient system [7] is now a well-studied chaotic system, as chaotic dynamics expected through a trophic coupling of three species [8]. More recently, an ocean ecosystem model also exhibits chaotic properties related to the external seasonal forcing [9]. In particular, the issues raised by chaos theory in ecology have been the subject of several reviews [10–15].

The compelling reasons for the emerging chaos theory in ecology is based on the hope that complex systems could be explained by relatively low-order processes. This leads to the development of a suite of algorithms aimed at the detection of chaotic behaviour and the classification of system dynamics [14,15]. While such approaches have been applied to a wide variety of time series [13,16,17], as to detect dynamic spatial chaos [18–20], the development of nonlinear thinking to marine ecology has a more recent history. Only a few studies have been devoted to detect chaotic signature in both marine time series and transects, and led to controversial results. Thus, Sugihara and May [21] found evidence for chaotic dynamics in time series of weekly diatom counts, and Scheffer [22] argued that chaotic deterministic dynamics should be commonplace in plankton communities. On the contrary, Ascioti et al. [23] and Strutton et al. [24,25] did not find any evidence of chaotic dynamics in both zooplankton and phytoplankton time series and phytoplankton transects, respectively.

More recently, a new field of marine research has been devoted to the stochastic characterization of intermittent processes in the framework of multifractals [26–34]. Multifractals, which has been recently reviewed by Pascual et al. [26] and Seuront et al. [32], can be regarded as a generalization of fractal geometry [35] initially introduced to describe the relationship between a given quantity and the scale at which it is measured. While fractal geometry describes the structure of a given descriptor with the help of only one parameter (i.e., the so-called fractal dimension), multifractals characterize its detailed variability by an infinite number of sets (roughly speaking, each of them corresponds to the fraction of space where data exceed a given threshold), each with its own fractal dimension. Such approaches, which do not require any statistical preconception on the data, provide very good approximations—at all scales and all intensities—of the statistics of an intermittently fluctuating descriptor, and determine the probability description of the descriptor values; see [26,32] for further details. Moreover, the statistical consequence of intermittency being a strong departure from Gaussianity [36], multifractals provide a powerful alternative to basic random walk models explicitly based on Gaussian statistics [37]. Thus, considering that in the general background of spatio-temporal intermittency encountered in the ocean [38], knowledge of the precise statistics of any intermittent fields may avoid the bias introduced by chronic undersampling of an intermittent signal [39], a stochastic multifractal framework is particularly well suited to describe the structure of quantities that vary intermittently [26,30–34].

Several misconceptions about chaos precisely pertain to its relationship to stochastic behaviour [14]. Chaos and stochasticity are nevertheless not equivalent: not only do the underlying mechanisms differ, but the consequences for observers are very different. In purely deterministic systems, predictions made from the governing equations will be perfect. Chaotic systems are predictable over short time scales because they are deterministic; the lack of predictive power over long time scales stems from the lack of complete information about the exact location of initial conditions. In contrast, purely stochastic systems are unpredictable over any time scales because of their probabilistic nature. In such approaches, the variability of a given descriptor is driven by "news" events, which represent exogenous variables—exogenous in the sense that they are not a part of an internal mechanism which drives the descriptor fluctuations. The branches of a tree move because of the wind, which is "exogenous" to the tree, and therefore "news" to it, whereas a chaotic model of the motion of trees would assume the existence of a simple deterministic 'nonlinear' engine within the tree (i.e., endogenous) which generates chaotic motion by a simple mechanism of feedback of the motion of the tree upon itself. Finally, the distinction between stochastic and deterministic dynamics has important practical implications. For instance, if fluctuations in population sizes are driven primarily by deterministic factors, and if those factors are understood, then the dynamics are predictable over short time scales. Management of such populations is feasible. On the other hand, if fluctuations are driven primarily by exogenous stochastic forces, then prediction and management become much more difficult.

Thus, given that deterministic equations in a small number of variables can generate complicated behaviour, the question arises: how much of the complicated behaviour observed in nature can be described by a small number of variables? This question has been widely addressed in the framework of turbulence. Ruelle and Takens [40] indeed showed that near the transition to turbulence, the many degrees of freedom of turbulence are coupled coherently, and lead to an enormous reduction in dimension (i.e., low-order deterministic chaos). However, both empirical and theoretical studies have demonstrated that fully developed turbulence [41–43] was rather characterized by its multifractal properties (i.e., high-order stochasticity). Previous empirical studies of phytoplankton and nutrient patchiness in turbulent environments [30–34] nevertheless suggested potential effects of both turbulence intensities and advective processes on the multifractal structure of both physical (i.e., temperature and salinity) and biological (i.e., phytoplankton biomass) parameters.

Such transitions between low-order deterministic chaos and high-order stochasticity might then be observed in the tidally mixed waters of the Eastern English Channel, where turbulence intensities may vary by more than two orders of magnitude over one tidal cycle [34,44], and is generally thought as driving phytoplankton biomass variability [30–32]. Herein, the goal of this paper is first to find out whether time series of physical (temperature and salinity) and biological (phytoplankton biomass) parameters recorded in tidally mixed waters are chaotic or not, second, to investigate the potential effects of differential tidal forcing on the chaotic and/or stochastic nature of the variables in question. Finally, we compare the chaotic and/or stochastic structure of purely passive scalars (i.e., temperature and salinity) with the one of phytoplankton biomass in order to infer the reality of referring to phytoplankton cells as passive

scalars. In order to identify potential chaotic signature, several complementary techniques of phase-space reconstruction were applied to temporal data from the marine environment. On the other hand, the stochastic structure of the data sets has been investigated using multifractal formalism.

2. Study area and sampling

The sampling experiment was conducted during 60 h (i.e., five tidal cycles) in a period of spring tide, from 28 to 30 March 1998, at an anchor station located in the coastal waters of the Eastern English Channel (50°47′300 N, 1°33′500 E). The tidal range in this system is one of the largest in the world, ranging from 3 to 9 m. Tides present a residual circulation parallel to the coast, with nearshore waters drifting from the English Channel into the North Sea. This coastal flow [45] is influenced by the fluvial supplies, distributed from the Bay of Seine to the Straits of Dover, and separated from offshore waters by a tidally controlled frontal area. It is characterized by its low salinity, turbidity, phytoplankton richness and productivity [45,46], and is separated from offshore waters by a tidally controlled frontal area [47,48]. Temperature, salinity and in vivo fluorescence were simultaneously recorded at 2 Hz from a single depth (5 m) with a SBE 25 Sealogger CTD (Conductivity–Temperature–Depth) probe, and a Sea Tech fluorometer, respectively. Every hour, samples of water were taken at 5 m depth to estimate chlorophyll *a* concentrations, which appear significantly correlated with in vivo fluorescence (Kendall's $\tau = 0.778$, $p < 0.01$). In the following, the latter parameter will then be regarded as a direct estimate of phytoplankton biomass. Because the main objective of this contribution is to investigate the potential effect of varying tidal forcing on the local structure of physical and biological parameters, the data analyzed here consist in 24 time series (labelled from S1 to S24) of 1 h duration (7200 data points) re-sampled from the original dataset in order to be representative of the different conditions of tidal current speed and direction, taken every 10 min, from the sampling depth (Table 1).

3. Methods

3.1. Data pre-processing

Time series analysis requires the assumption of at least reduced stationarity, i.e., the mean and the variance of a time series depend only on its length and not on the absolute time [49]. The existence and the significativity of any potential linear trends was testing calculating Kendall's τ correlation which does not require any hypothesis about the characteristics of the original dataset distribution (Kendall's coefficient of correlation was used in preference to Spearman's coefficient of correlation ρ because Spearman's ρ gives greater weight to pairs of ranks that are further apart, while Kendall's τ weights each disagreement in rank equally, see [50] for further developments). We then eventually detrended time series fitting linear regressions to the original data by

Table 1
Tidal conditions, water column depth and mean values of temperature, salinity and in vivo fluorescence for the 24 studied data sets

	Tidal current		Depth	T	S	F
	Speed (m s^{-1})	Dir (°)				
S1	0.55	240	21.56	6.55	34.60	18.32
S2	0.45	220	22.49	6.53	34.60	15.20
S3	0.10	60	27.38	6.51	34.62	10.90
S4	0.95	15	28.28	6.50	34.66	9.39
S5	0.90	10	26.21	6.49	34.70	8.23
S6	0.15	10	23.25	6.51	34.65	10.25
S7	0.32	260	21.52	6.53	34.61	15.02
S8	0.62	230	22.21	6.52	34.62	17.24
S9	0.10	85	27.19	6.50	34.65	11.45
S10	0.98	10	28.47	6.49	34.72	6.80
S11	1.00	10	26.53	6.49	34.67	7.29
S12	0.30	10	23.66	6.50	34.64	11.00
S13	0.35	290	21.38	6.53	34.62	17.40
S14	0.30	200	21.72	6.55	34.62	15.82
S15	0.11	140	26.19	6.52	34.66	13.46
S16	0.80	10	28.65	6.5	34.69	10.75
S17	1.10	10	27.15	6.49	34.70	6.64
S18	0.40	10	24.15	6.51	34.68	7.35
S19	0.35	260	21.75	6.53	34.63	12.64
S20	0.87	250	21.68	6.55	34.62	17.69
S21	0.73	230	25.23	6.55	34.61	15.16
S22	0.18	10	28.65	6.53	34.71	8.30
S23	1.04	10	27.50	6.50	34.66	5.37
S24	0.60	10	25.95	6.50	34.62	3.87

least squares and used the regression residuals in further analysis. The purpose of this is to eliminate aliasing in further analysis due to large scale structures present in the data sets, such as in monotonically increasing or decreasing trends. In order to provide direct comparisons between the different parameters, the time observations, y_i, were converted into normalized, dimensionless descriptors, x_i, following:

$$x_i = \frac{y_i - y_{\min}}{y_{\max} - y_{\min}} , \tag{1}$$

where $y_{\max}$ and $y_{\min}$ are the maximum and minimum values of the series, respectively. Samples of the resulting time series are given in Fig. 1.

3.2. The search for deterministic chaos

In the following our datasets are regarded as finite sets of time observations, x_i, taken at regular intervals, 0.5 s for temperature, salinity and in vivo fluorescence time series:

$$X_i = \{x(1), x(2), x(3), \ldots, x(N_{obs})\} , \tag{2}$$

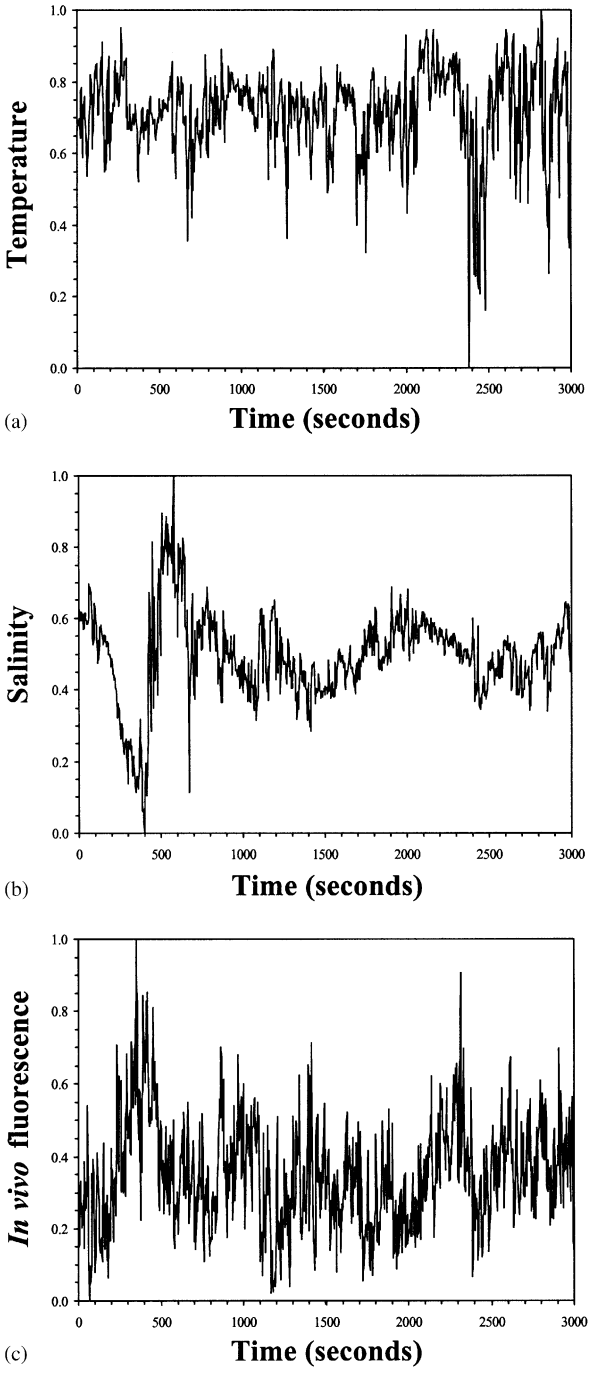

Fig. 1. Normalized temperature (a), salinity (b) and in vivo fluorescence (c) time series recorded in the Eastern English Channel, shown for data set S1.

where N_{obs} is the total number of observations in each set. The time length of any observed period, T, is related to N_{obs} as

$$T = N_{obs}\Delta t \ . \tag{3}$$

More specifically, the three methods used here to investigate the properties of our sets, i.e., the PTM [51,52], Lyapunov exponents estimates [53], and the correlation integral method [54], are based on the assumption that the dynamics of any underlying dynamical systems can be described in some multidimensional phase-space from the knowledge of the time series of a single observation $x(t)$ by constructing E-dimensional vectors defined by:

$$\vec{X}(t) = (x(t), x(t-\tau), \ldots, x(t-(E-1)\tau) \ , \tag{4}$$

where E is the embedding dimension (i.e., the dimension of the vectors), and $\tau = p\Delta t$ is the lag (i.e., the number of data points separating each of the vector's elements). As an example, one can observe that for $E = 3$ and $\tau = 1$, the vector $\vec{X}(t)$ consists of $x(t)$ and the $E-1$ immediately preceding points of the time series (i.e., the set of vectors $\{\vec{X}(3), \vec{X}(4), \ldots, \vec{X}(n)\}$ is denoted as $\{(x(3), x(2), x(1)), ((x(4), x(3), x(2)), \ldots, ((x(n), x(n-1), (x(n-2))\}$).

In the above case, the delay time τ must be chosen so as the result in points that are not correlated to previously plotted points. Thus, a first choice of τ should be in terms of the decorrelation time of the time series [55]. A straightforward procedure is to consider the decorrelation time equal to the lag at which the autocorrelation function for the first time attains the value of zero. One may also note here that no averaging nor filtering have been employed since it is known that such data manipulations can obscure the presence of chaos [13].

3.2.1. The Packard–Takens method (PTM)

Dissipative dynamical systems which exhibit chaotic behaviour often have a strange attractor in phase-space [54]. It is for instance the case for the movements of atmospheric flows which produce a specific phase-space trajectory now widely known as the Lorentz's attractor [56]. More precisely, a strange attractor has orbits that lie within a defined region of phase-space but the orbits never intersect and never follow the same trajectory twice.

The phase-space attractor of a system is then a map of the changing conditions in the system: each point on the attractor is a summary of all the variables affecting the system at a moment in time. As the system evolves, changes in the variables result in a different location of the point in phase-space. The points in phase-space trace a trajectory that summarizes the changes of the system. Three-dimensional phase-space diagrams of the attractor describing the time series were produced using the 'time delay' method [51]. In practice, the one-dimensional time series, and thus all the factor affecting it, can be represented by the trajectory of points in three-dimensional phase-space. The attractor is created by plotting each value as a function of its preceding value, or in other words, from the plot of $x(t+1)$ vs. $x(t)$, where x is the actual value (in our case the normalized, dimensionless descriptors) and t the index of the point. It can be noticed here that an attractor with a regular shape will also emerge in plots using $x(t+2)$ or

$x(t+3)$ for example, or $x(t+n)$, with many n. This procedure was repeated for each successive point in the time series and the resultant points were connected producing the phase-space trajectory.

3.2.2. Largest Lyapunov exponents (LLE)

The limits of predictability are set by how fast the trajectories diverge from nearby initial conditions. This feature is quantified by Lyapunov exponents which are the average exponential rates of divergence or convergence of nearby orbits in phase-space. Any systems containing at least one positive Lyapunov exponent is defined to be chaotic, with the magnitude of the exponent reflecting the time scale at which the system dynamics become unpredictable. In other words, the larger the positive exponent, the more chaotic the system, and the shorter the time scale of system predictability [53].

To define the Lyapunov exponents, imagine an infinitesimal hypersphere of initial conditions in the n-dimensional phase-space. There is one Lyapunov exponent for each degree of freedom of the system. We observe the evolution of the hypersphere as time progresses. The hypersphere will be deformed into a hyper-ellipsoid because the evolution of the system. Then the ith Lyapunov exponent can be defined in terms of the length of the ith principal axis, p_i, of the ellipsoid as

$$\lambda_L = \lim_{\tau\to\infty} \frac{1}{\tau} \ln \frac{p_i(\tau)}{p_i(0)} , \tag{5}$$

where the λ_L are ordered from largest to smallest in an algebraic sense [53,57]. A minimum condition for chaos is that the LLE, λ_L, is positive.

In practice, we used an algorithm developed to estimate the LLE, λ_L, from a time series by using a relatively simple procedure [53], and which has been demonstrated to be robust over a large range of input parameters and relatively accurate for small, noisy data sets [57]. The delay time τ was chosen as the decorrelation time of the time series, as previously mentioned. We carried the embedding dimension E from 2 to 10.

3.2.3. Correlation integral algorithm (CIA)

While the LLE is used to estimate the limits of predictability of a given time series, the complementary CIA is devoted to the quantitative characterization of the attractor of the series. As previously demonstrated [52], an attractor topologically equivalent to the attractor of the system producing the data is obtained for every value of τ and for E sufficiently greater than the fractal dimension, i.e., $E \geqslant (2D+1)$.

From the new multidimensional time series defined by Eq. (4), the correlation integral [54] is defined as:

$$C(r) = \lim_{N\to\infty} \frac{1}{N^2} \sum_{j=1}^{N} \sum_{i=j+1}^{N} \theta(r - |\vec{X}_i - \vec{X}_j|) , \tag{6}$$

where $N = N_{obs} - p(n-1)$ is the number of distinct pairs in the embedding space, $|\vec{X}_i - \vec{X}_j|$ is the Euclidean distance operator between the ith and jth sample, r is an arbitrary time called 'lag time' (distance between vectors), and $\theta(\xi)$ is the Heaviside

function, defined as follows:

$$\theta(\xi) = \begin{cases} 0 & \text{for } \xi < 0 \\ 1 & \text{for } \xi \geqslant 0 \,. \end{cases} \tag{7}$$

The correlation integral $C(r)$ represents the probability that the distance between a pair of randomly chosen points on the E-dimensional reconstruction will be less than a distance r apart [54]. In the case of random processes, the phase-space trajectory is directly linked to the volume of the considered E-dimensional space as:

$$C(r) \underset{r \to 0}{\propto} r^{E} \,, \tag{8}$$

while for an attractor the phase-space trajectory is more compact and the correlation integral is then characterized by its following scaling properties:

$$C(r) \underset{r \to 0}{\propto} r^{v} \,, \tag{9}$$

where the exponent v is the correlation exponent (or correlation dimension); it can be estimated as the slope of the log–log plot of $C(r)$ vs. r, using a simple least square method.

For chaotic data, v will approach a constant value as the embedding dimension E is increased. That constant value is an estimate of the correlation dimension which measures the local structure of the strange attractor. The dimension v of the strange attractor indicates at least how many variables are necessary to describe evolution in time. For instance, $v = 2.5$ indicates that a given time series can be described by a system equation containing three independent variables.

3.3. High dimensionality and multifractal structure

As was implied in the introduction, high frequency fluctuations in the tidally mixed coastal waters of the Eastern English Channel are far from Gaussian. Multifractal distributions have this property, and they apply to signals with scaling characteristics [58,59], as the one studied here may well have, as previously shown from the multifractal properties of temperature, salinity and phytoplankton biomass in similar areas [30–32,34]. Moreover, recent studies have demonstrated that multifractal processes generally lead to universal multifractals with generators characterized by only three parameters H, C_1, and α [60,61]. $H (0 \leqslant H \leqslant 1)$ characterizes the degree of non-conservation of the process (i.e., $H = 0$ for stationary process). C_1 is the codimension that characterizes the sparseness of the process, and satisfies $0 \leqslant C_1 \leqslant 1$ for time series: $C_1 = 0$ for a homogeneous process and C_1 is all the more high as the process is sparse, indicating that the field values corresponding to any given level of variability are more scarce. The index α, called the Lévy index, is the degree of multifractality bounded between $\alpha = 0$ and $\alpha = 2$ corresponding to the monofractal case and to the maximum, or log-normal, multifractal case, respectively. As α increases, the more numerous are the variability levels bounded between lower and higher values of the descriptor [32].

There are several ways to estimate the universal parameter values. The parameters H, C_1 and α can thus be estimated considering different derivation of the qth order structure functions, which can be regarded as a statistical generalization of the power spectral analysis to higher order of moments [30–32,34,62–65], but also from the Double Trace Moment technique [66–69], a very specific data analysis technique which has been extensively explained elsewhere [32]. In the following, we only report the results of the analysis process, for further explanations and details one may refer to a recent review [32] wholly devoted to the introduction of universal multifractal concepts and their related analysis techniques to marine ecology. More details on the universal multifractal theoretical background can also be found in [41,60,61,70], Finally, for a detailed discussion of what can be ecologically concluded from the use of multifractal algorithms, one may refer to [32].

4. Results

4.1. Phase-space diagrams

The delay time τ has been chosen as the decorrelation time of the time series [55] as 75, 105 and 25 s for temperature, salinity and in vivo fluorescence time series, respectively (not shown). This delay time was also used for the following calculations of Lyapunov exponents and correlation dimensions.

The phase-space portraits of the attractors produced by the PTM did not clearly exhibit any attractor (Fig. 2). Nevertheless, one may note clear differences between the phase-space trajectories of in vivo fluorescence on the one hand and temperature and salinity on the other hand. Indeed, the phase-space trajectories for temperature and salinity appear as somewhat elongated and relatively narrow spatial distribution (Fig. 2a, b). On the contrary, phase-space trajectories of in vivo fluorescence did not exhibit any characteristic shape, suggesting a more space filling—or 'random'—behaviour (Fig. 2c). Moreover, comparison of phase-space trajectories obtained from time series recorded in high and low hydrodynamic conditions leads to further results. Phase-space trajectories of temperature and salinity then appear clearly more structured in lower hydrodynamic conditions (Fig. 2d, e), while the apparent randomness of in vivo fluorescence phase-space trajectories remains whatever the hydrodynamic conditions (Fig. 2f).

4.2. Largest Lyapunov exponents

The LLE, λ_L, calculated over a range of embedding dimensions E exhibit clearly different behaviours (Fig. 3). By embedding dimension 8, the temperature and salinity LLE converge to positive values which are all the more large that the hydrodynamic conditions are high (Fig. 3a, b). In other words, the higher are the hydrodynamic conditions, the larger the positive exponent, the more chaotic the system, and the shorter the time scale of system predictability [53], This is confirmed by the significant negative correlation between LLE of both temperature and salinity, and tidal current

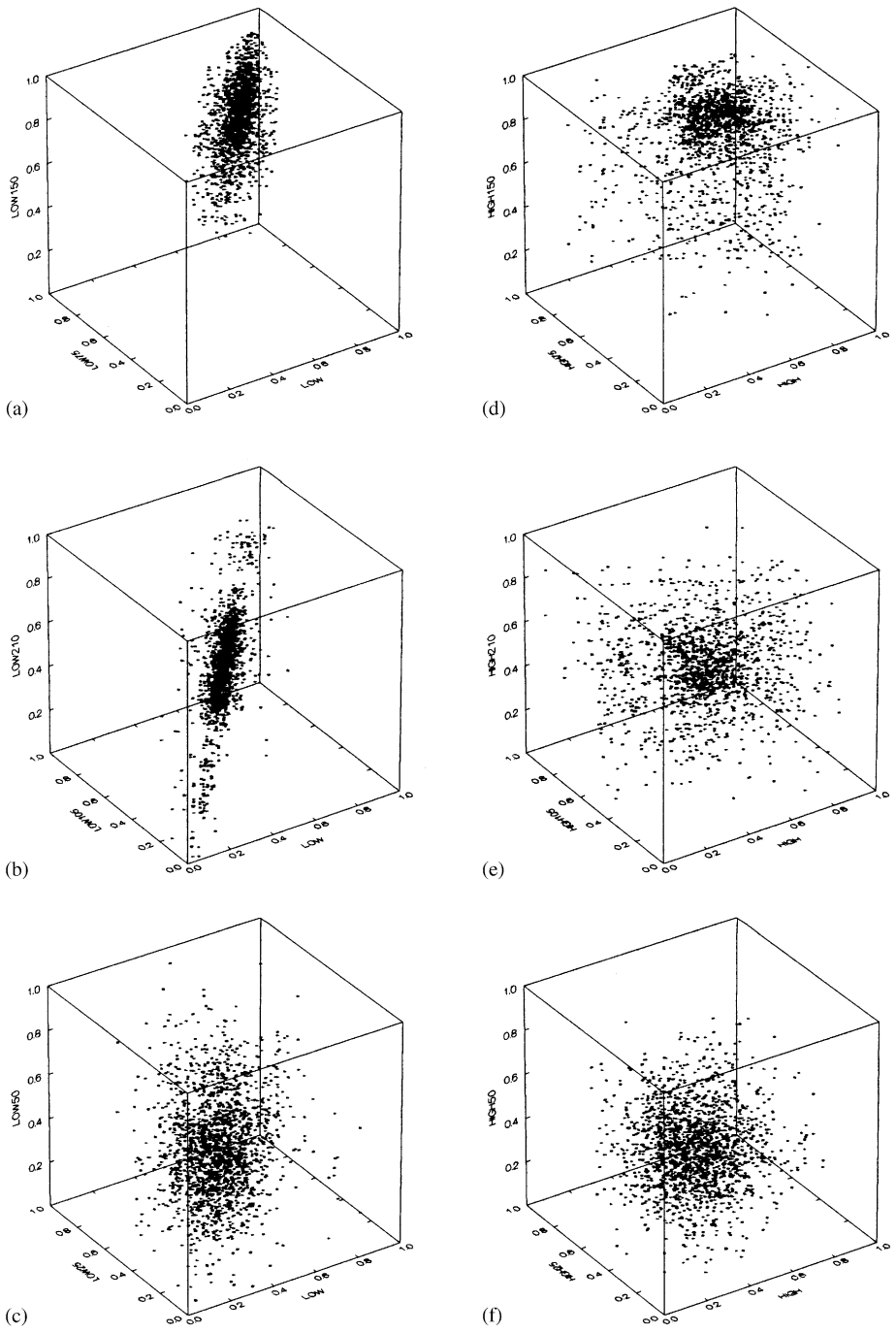

Fig. 2. Three-dimensional phase-space trajectories for temperature, salinity and in vivo fluorescence in low (a, b, c; S9) and high (d, e, f; S11) hydrodynamic conditions.

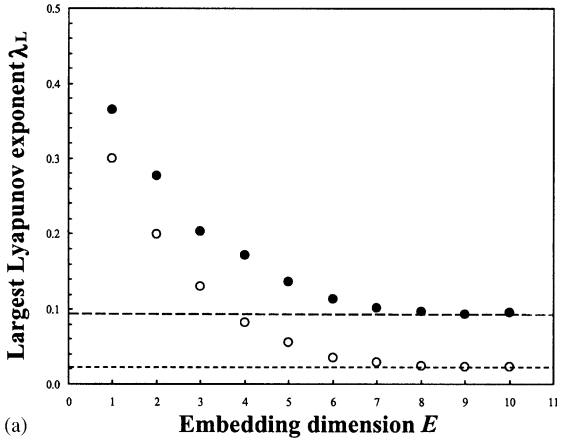

(a)

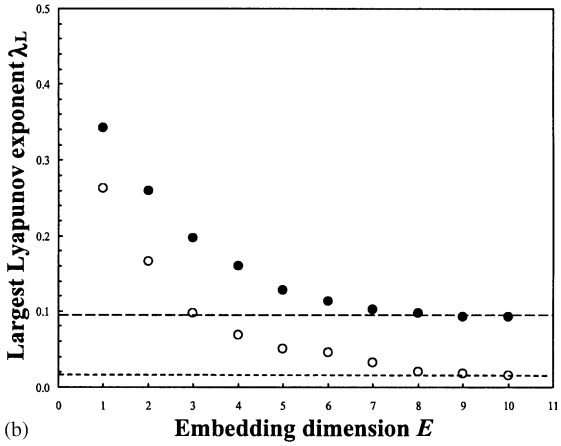

(b)

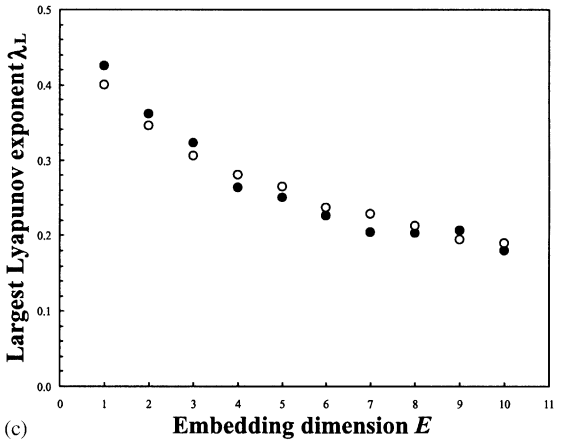

(c)

Fig. 3. The LLE λ_L estimates for temperature (a), salinity (b) and in vivo fluorescence (c) in high (black circles; S15) and low (open circles; S23) hydrodynamic conditions.

Table 2
The LLE λ_L estimates for temperature, salinity and in vivo fluorescence from the 24 available data sets, and the related time scale of system predictability

	λ_L			Predictability (second)		
	T	*S*	*F**	*T*	*S*	*F*
S1	0.048	0.045	0.212	20.83	22.22	4.72
S2	0.044	0.043	0.223	22.73	23.26	4.48
S3	0.012	0.009	0.225	83.33	111.11	4.44
S4	0.098	0.105	0.243	10.20	9.52	4.12
S5	0.092	0.094	0.172	10.87	10.64	5.81
S6	0.021	0.023	0.221	47.62	43.48	4.52
S7	0.031	0.035	0.236	32.26	28.57	4.24
S8	0.055	0.057	0.198	18.18	17.54	5.05
S9	0.011	0.009	0.217	90.91	111.11	4.61
S10	0.091	0.088	0.171	10.99	11.36	5.85
S11	0.095	0.084	0.223	10.53	11.90	4.48
S12	0.038	0.039	0.181	26.32	25.64	5.52
S13	0.041	0.039	0.234	24.39	25.64	4.27
S14	0.042	0.039	0.182	23.81	25.64	5.49
S15	0.012	0.016	0.234	83.33	62.50	4.27
S16	0.076	0.079	0.172	13.16	12.66	5.81
S17	0.121	0.133	0.228	8.26	7.52	4.39
S18	0.038	0.041	0.196	26.32	24.39	5.10
S19	0.032	0.034	0.253	31.25	29.41	3.95
S20	0.085	0.088	0.228	11.76	11.36	4.39
S21	0.076	0.074	0.234	13.16	13.51	4.27
S22	0.025	0.017	0.254	40.00	58.82	3.94
S23	0.097	0.096	0.174	10.31	10.42	5.75
S24	0.071	0.075	0.187	14.08	13.33	5.35
Mean	0.056	0.057	0.212	28.53	30.06	4.79
SD	0.032	0.033	0.027	24.36	28.84	0.64
Min	0.011	0.009	0.171	8.26	7.52	3.94
Max	0.121	0.133	0.254	90.91	111.11	5.85

*Following the absence of convergent behaviour for the fluorescence Lyapunov exponents, we reported here the λ_L estimated for $E = 10$.

speed direction. The LLE and the associated time scale of predictability are shown in Table 2.

On the contrary, whatever the hydrodynamic conditions, in vivo fluorescence LLE remain significantly higher than temperature and salinity LLE, indicating more chaotic behaviour and less predictability, but never converge to any constant value, even when the embedding dimension E is increased up to 10 (Fig. 3c).

4.3. Correlation integral

Fig. 4 show the correlation integral $C(r)$ on logarithmic scales as a function of distance r by varying embedding dimension E from 1 to 10. Estimates of the correlation

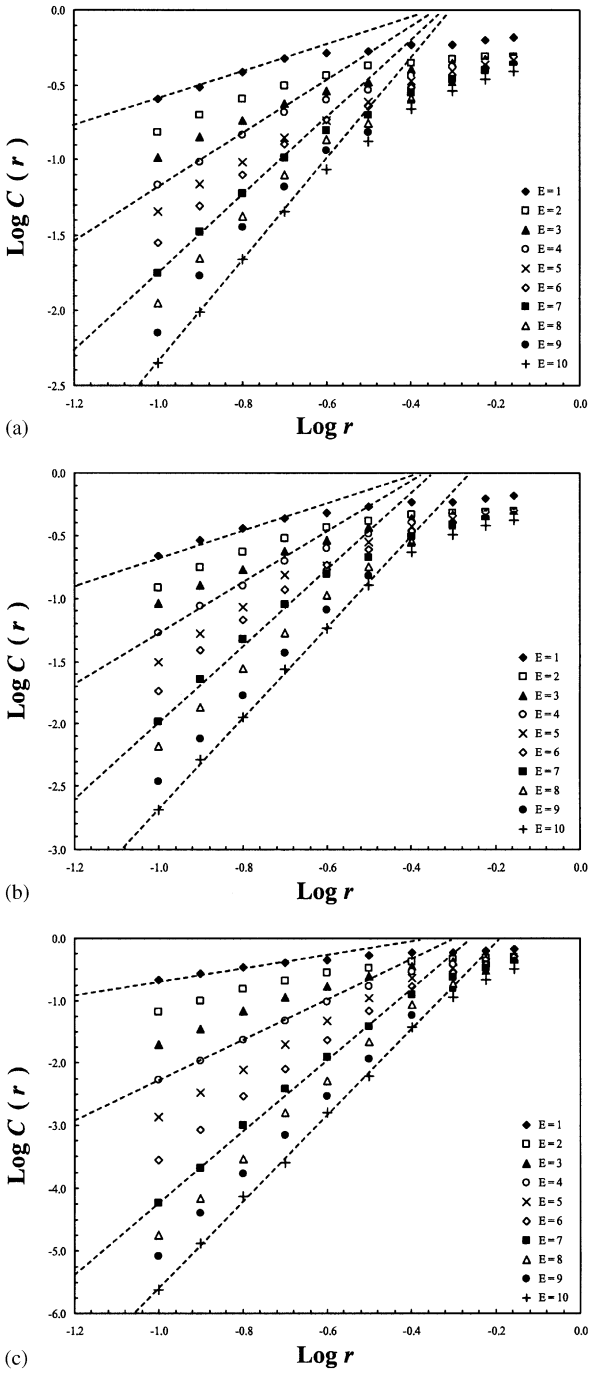

Fig. 4. Log–log plots of correlation integral $C(r)$ versus distance r for various embedding dimensions E for temperature (a), salinity (b) and in vivo fluorescence (c), shown for database S8.

Table 3
Empirical estimates of the universal multifractal parameters H, C_1 and α for temperature, salinity and in vivo fluorescence for the 24 studies data sets

	Temperature			Salinity			In vivo fluorescence		
	H	C_1	α	H	C_1	α	H	C_1	α
S1	0.38	0.040	1.90	0.37	0.049	1.88	0.38	0.042	1.84
S2	0.36	0.040	1.85	0.35	0.050	1.84	0.43	0.059	1.80
S3	0.35	0.056	1.87	0.32	0.070	1.86	0.61	0.137	1.76
S4	0.34	0.050	1.86	0.32	0.050	1.86	0.45	0.056	1.90
S5	0.37	0.050	1.84	0.36	0.060	1.85	0.45	0.052	1.88
S6	0.37	0.060	1.84	0.36	0.050	1.89	0.58	0.135	1.75
S7	0.38	0.050	1.87	0.40	0.060	1.88	0.46	0.087	1.79
S8	0.36	0.060	1.86	0.38	0.050	1.87	0.37	0.052	1.83
S9	0.38	0.050	1.83	0.39	0.060	1.85	0.50	0.098	1.76
S10	0.35	0.040	1.88	0.40	0.031	1.88	0.46	0.073	1.92
S11	0.40	0.050	1.84	0.40	0.060	1.86	0.46	0.071	1.93
S12	0.36	0.048	1.86	0.40	0.057	1.89	0.45	0.058	1.79
S13	0.35	0.040	1.86	0.37	0.050	1.88	0.45	0.054	1.79
S14	0.36	0.050	1.85	0.35	0.060	1.86	0.46	0.068	1.79
S15	0.28	0.053	1.86	0.29	0.062	1.89	0.49	0.096	1.76
S16	0.37	0.060	1.85	0.36	0.060	1.86	0.40	0.077	1.78
S17	0.38	0.040	1.84	0.36	0.050	1.87	0.38	0.068	1.96
S18	0.36	0.050	1.88	0.36	0.060	1.88	0.43	0.073	1.78
S19	0.35	0.050	1.85	0.36	0.060	1.84	0.45	0.064	1.79
S20	0.42	0.060	1.89	0.34	0.070	1.91	0.40	0.054	1.88
S21	0.41	0.070	1.91	0.39	0.060	1.90	0.41	0.055	1.86
S22	0.36	0.057	1.90	0.35	0.070	1.85	0.60	0.120	1.75
S23	0.30	0.032	1.87	0.30	0.052	1.9	0.49	0.081	1.90
S24	0.34	0.050	1.89	0.36	0.040	1.89	0.55	0.091	1.76
Mean	0.36	0.050	1.86	0.36	0.056	1.87	0.46	0.076	1.82
SD	0.03	0.008	0.02	0.03	0.009	0.02	0.07	0.026	0.06
Max	0.42	0.070	1.91	0.40	0.070	1.91	0.61	0.137	1.96
Min	0.28	0.032	1.83	0.29	0.031	1.84	0.37	0.042	1.75

Min: minimum values, *Max*: maximum values, *SD*: standard deviation.

dimension v (see Eq. (9)) for temperature and salinity did not converge to any constant value whatever the hydrodynamic conditions (Fig. 5a, b), and indicate the lack of empirical evidence for deterministic chaos. Moreover, no significant differences can have been observed between temperature and salinity correlation dimensions, nor between the different time series for either parameter, suggesting very similar behaviours of temperature and salinity time series in phase-space.

The results for in vivo fluorescence time series are very similar with those of temperature and salinity. Clearly no saturation, and therefore no evidence of low-order deterministic chaos, exist whatever the hydrodynamic conditions (Fig. 5c). As previously shown for temperature and salinity time series, no significant differences exist between the correlation dimensions v. These results confirm the previous lack of convergence

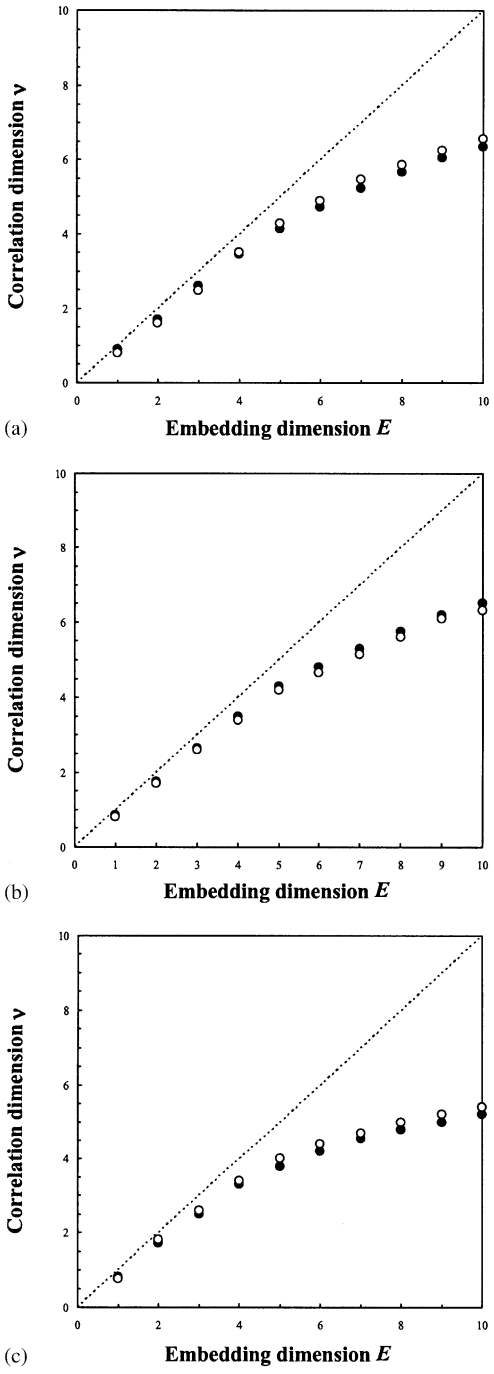

Fig. 5. Correlation dimensions ν versus embedding dimensions E for temperature (a), salinity (b) and in vivo fluorescence (c) in high (black circles; S15) and low (open circles; S23) hydrodynamic conditions.

of the LLE (see Fig. 3c), and indicate that there is no evidence for deterministic chaos in the temporal fluctuations of phytoplankton biomass time series.

4.4. Multifractal structure

Values of the universal multifractal parameters H, C_1 and α estimated for temperature, salinity and in vivo fluorescence time series are shown in Table 3. More precisely, there were significant differences between temperature, salinity and fluorescence H values. Fluorescence parameters were significantly greater than temperature and salinity which remain indistinguishable. The fractal codimensions C_1 lead to different results: temperature, salinity and in vivo fluorescence codimensions C_1 thus cannot be statistically distinguished. Finally, the parameters α also cannot be distinguished for temperature, salinity and in vivo fluorescence (Table 3).

Nevertheless, correlation analyses conducted in order to infer any potential causality between the structure of temperature, salinity and in vivo fluorescence time series and both physical (i.e., current speed and direction) and biological (i.e., in vivo fluorescence means and standard deviations) parameters (Table 4) lead to further results. It was then found that the universal parameters (i.e., H, C_1 and α) estimated for temperature and salinity time series were neither significantly correlated with current speed nor direction, indicating a relative homogeneity in the small-scale temporal structure of these purely passive scalars. On the contrary, the universal multifractal parameters characterizing in vivo fluorescence variability were significantly correlated with both current speed and direction. More precisely, phytoplankton biomass distributions are more conservative (i.e., low H values) and less sparse (i.e., low C_1 values) both during ebb tide and in high hydrodynamic conditions, while the Lévy index α (i.e., the hierarchy of variability levels present in the phytoplankton biomass distribution) increases with current speed. Moreover, the multifractal parameters (i.e., H, C_1 and α) are not correlated to means and standard deviations (i.e., variability) for phytoplankton biomass time series.

5. Discussion and concluding remarks

We have presented here empirical evidence that purely passive tracers of the flow (temperature and salinity), as well as biological tracers such as phytoplankton cells never exhibit signature for low-order deterministic chaos, whatever the intensity of turbulence. On the opposite, the time series investigated clearly exhibited high-order stochastic properties. In addition, the stochastic structure of purely passive scalars (i.e., temperature and salinity) remained invariant, while the one of phytoplankton biomass must be regarded as highly structured in time by both hydrodynamic and advective processes. We discussed hereafter (i) the relevance of the data analysis techniques used to infer the existence of deterministic chaos and stochastic behaviour, especially in the context of short time series that are the rule in most of ecological studies, and (ii) the implications of our findings on the future of modelling approaches in marine ecology.

Table 4
Correlation matrix of variables relative to the structure of temperature, salinity and in vivo fluorescence time series

	C_{speed}	C_{Dir}	Depth	T	S	F	SD_T	SD_s	SD_F	H_T	H_S	H_F	C_{IT}	C_{IS}	C_{IF}	α_T	α_S	α_F
C_{speed}	1.000	—	—	—	—	—	—	—	—	—	—	—	—	—	—	—	—	—
C_{Dir}	−0.251	1.000	—	—	—	—	—	—	—	—	—	—	—	—	—	—	—	—
Depth	0.315	−0.787**	1.000	—	—	—	—	—	—	—	—	—	—	—	—	—	—	—
T	−0.350	0.824**	−0.672**	1.000	—	—	—	—	—	—	—	—	—	—	—	—	—	—
S	0.351	−0.746**	0.728**	−0.660**	1.000	—	—	—	—	—	—	—	—	—	—	—	—	—
F	−0.330	0.893**	−0.734**	−0.734**	−0.689**	1.000	—	—	—	—	—	—	—	—	—	—	—	—
SD_T	0.576**	−0.496*	0.440*	−0.455*	0.026	−0.746**	1.000	—	—	—	—	—	—	—	—	—	—	—
SD_S	0.690**	−0.185	0.009	−0.213	−0.260	−0.416*	0.833**	1.000	—	—	—	—	—	—	—	—	—	—
SD_F	0.110	−0.140	−0.135	0.100	−0.360	−0.073	0.539**	0.649**	1.000	—	—	—	—	—	—	—	—	—
H_T	0.202	0.223	−0.252	0.267	−0.149	0.291	−0.398	−0.028	−0.475*	1.000	—	—	—	—	—	—	—	—
H_S	0.048	0.102	−0.214	−0.040	−0.034	0.095	−0.306	0.015	−0.376	0.636**	1.000	—	—	—	—	—	—	—
H_F	−0.520**	−0.405*	0.336	−0.187	0.123	−0.415*	0.043	−0.330	−0.120	−0.329	−0.242	1.000	—	—	—	—	—	—
C_{IT}	−0.235	0.086	0.006	0.274	−0.107	0.230	−0.150	−0.213	−0.320	0.405 *	0.115	0.102	1.000	—	—	—	—	—
C_{IS}	−0.360	0.135	−0.037	0.330	−0.075	0.243	−0.079	−0.108	−0.146	0.240	−0.211	0.165	0.500	1.000	—	—	—	—
C_{IF}	−0.529**	−0.408*	0.378	−0.210	0.189	−0.364	0.174	−0.204	0.058	−0.246	−0.250	0.881**	0.241	0.248	1.000	—	—	—
α_T	0.048	0.201	−0.058	0.492*	−0.204	0.142	0.103	0.204	0.104	0.109	0.048	−0.019	0.212	−0.005	−0.118	1.000	—	—
α_S	0.141	0.059	−0.174	0.171	−0.196	0.067	0.391	0.168	0.089	0.012	−0.021	−0.078	0.088	−0.114	−0.047	0.507	1.000	—
α_F	0.901**	−0.155	0.233	−0.287	0.313	−0.219	0.294	0.566**	0.139	0.246	0.092	−0.501*	−0.324	−0.296	−0.517*	−0.021	0.118	1.000

C_{speed} and C_{Dir}: current speed and direction; SD_T, SD_S and SD_F: standard deviation of temperature, salinity and fluorescence time series; the subscript T, S and F associated to the parameters H, C_1 and α respectively identify temperature, salinity and fluorescence universal multifractal structures.

*: 5% confidence level.

**: 1% confidence level.

5.1. Searching for determinism and stochasticity in ecological time series

The PTM: a qualitative prerequisite in the search for chaos.

The PTM method is probably the faster and most direct method to infer the potential existence of deterministic chaos. Creating the phase-space attractor of a system with a computer is indeed a very simple task. All that is needed is the copy of the data file, paste it shifted by one, two or more places, and plot the data. Thus, a subjective assessment of the 'degree of randomness' can be reached almost instantaneously from this kind of plot. It is nevertheless evident here (see Fig. 2) that the characteristic shape of the attractor is not easy to describe in simple terms. Fig. 2 shows projections of phase-space trajectories onto three-dimensional space, so that the fact that no attractors can be seen does not imply that they do not exist when embedding in higher dimensional space. However, a strange attractor of higher-dimensional space often reflects its shape onto the lower dimensional space as well. For instance, the trajectory onto the two-dimensional phase-space [embedding dimension $E = 2$ in Eq. (4)] reconstructed from the time series of variable x of the Lorenz equations [56,71,72] shows a clear strange attractor. These results can then rather be regarded as a qualitative prerequisite analysis and demonstrate that inferring the existence of any deterministic structure beyond the highly fluctuating behaviour exhibiting by temperature, salinity and in vivo fluorescence time series (Fig. 1) is a far more difficult task.

5.1.1. LLEs and the 'edge of chaos'

The LLE estimates quantitatively confirm the subjective results of the PTM, i.e., a lower dimensional behaviour in low hydrodynamic conditions for temperature and salinity time series, and a higher dimensional behaviour for phytoplankton biomass time series which did not exhibit any convergent behaviour of their LLE for values of the embedding dimension E up to 10 whatever the hydrodynamical conditions. What may be regarded as being very important for ecologists is that, unlike fractal dimensions, Lyapunov exponents remain well defined in the presence of dynamical noise and can be estimated by methods that explicitly incorporate noise [73,74]. This leads to consider that estimating Lyapunov exponents is the best approach for detecting chaos in ecological systems [14]. One must nevertheless note some limitations of Lyapunov exponent estimates to detect deterministic chaos, lying both in estimates accuracy and the minimum number of data points required in the analysis. First, although the algorithm used in this paper [53] provides a good estimation of the LLEs for noise-free synthetically generated time series from chaotic dynamics, the estimation for experimental time series is still relatively imprecise [75]. Second, it has been stressed that to detect a chaotic attractor of dimension 3, at least 1000–30,000 data points are needed [53], while others [76] found that 5000 data points is a lower bound for the detection of chaos on some simple dynamical systems known to display chaotic behaviours in certain regimes. Moreover, Vassilicos et al. [77] demonstrated how the tests for chaos can give positive answers, e.g. positive Lyapunov exponents, when subsamples with smaller number of data points are used, and how these Lyapunov exponents converge to zero when the number of data points is increased.

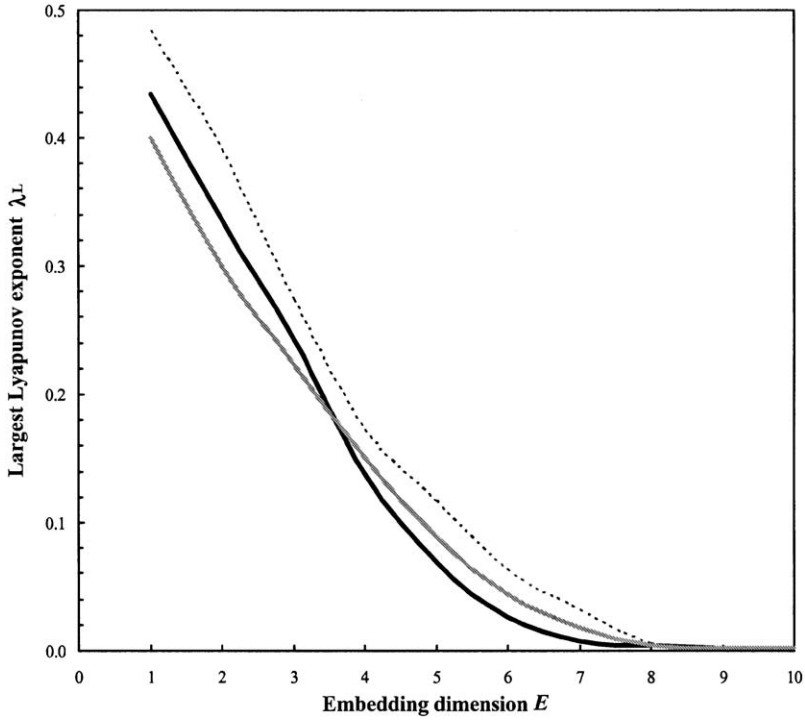

Fig. 6. The LLE λ_L estimates for temperature (continuous black line), salinity (dashed line) and in vivo fluorescence (continuous grey line) from the original 172,800 data points time series.

In order to confirm these results, we estimated the LLEs of the larger original time series (i.e., 172,800 data points) of temperature, salinity and in vivo fluorescence that were divided into 24 subsections of 7200 points in the present work. Subsequent results (Fig. 6) then indicated that LLE of temperature, salinity and phytoplankton biomass time series remain positive, but converge to zero. As previously mentioned, positive LLE indicates chaotic dynamics, but values quite close to zero should therefore only be interpreted as an order of magnitude. As a consequence, the different convergent positive values of the different LLE estimated for temperature and salinity time series in high and low hydrodynamic conditions (Fig. 3a, b) suggest a phenomenological shift between low dimensional chaos and high dimensional stochasticity as the one observed by Ruelle and Takens [40] near the transition to turbulence. Alternatively, a positive LLE close to zero can be interpreted as having been derived from a stochastic time series with many degrees of freedom [78]. More generally, one may note that systems with a Lyapunov exponent of zero are associated with a state called the edge of chaos, where complex behaviour is the rule. The exact meaning of the edge of chaos depends on the context within which it is used, but roughly speaking, it describes the vicinity of some instability point separating a region of more ordered (or less random) behaviour, from a region of less ordered (or more random) behaviour. The edge of

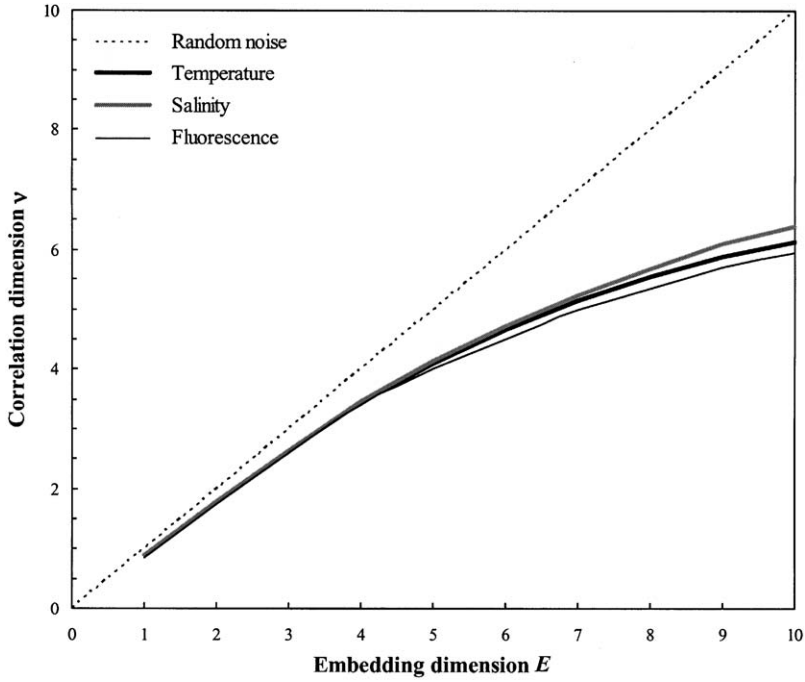

Fig. 7. Correlation dimensions v estimates versus embedding dimensions E for temperature, salinity and in vivo fluorescence from the original 172,800 data points time series.

chaos has indeed attracted considerable interest among biologists and ecologists in the last few years because processes such as evolution or adaptative behaviour have been precisely shown to be just at the edge of chaos [79–81]. Such a critical state would increase the adaptative efficiency of a given system, for instance in response to fluctuating environmental conditions, and could then be of prime interest in the future understanding of ecosystems functioning.

5.1.2. Correlation integrals

While Smith [82] has showed that if the data set is small, the correlation dimension v (see Eq. (9)) appears to converge towards a finite value even in the absence of chaos, this is obviously not the case in our case (Fig. 5). Moreover, correlation dimension v estimates for the 172,800 data points time series (Fig. 7) did not converge to any constant value, and confirm the lack of empirical evidence for deterministic chaos previously shown with smaller time series (Fig. 7). Our results then cannot be associated with sampling limitation. A correlation dimension of 2 has thus been identified on the basis of a 1200 values chlorophyll transect recorded in the central waters of the Ligurian Sea (NW Mediterranean Sea) [83]. This result then confirms the efficiency of the correlation algorithm to detect low deterministic chaos when applied to small data sets. This also suggests—as previously done in this paper—that different hydrodynam-

ical conditions might be at the origin of differential space–time structures, in terms of low-order deterministic chaos or high-order stochasticity. Then, high hydrodynamic conditions, as those occurring in the Eastern English Channel, could be at the origin of temperature, salinity and phytoplankton biomass distributions characterized by their high-order stochasticity, while in low hydrodynamic conditions, as those encountered in the stable waters of the Ligurian Sea, phytoplankton distribution could be rather characterized by a low-order deterministic behaviour.

While our results suggest that temperature, salinity and phytoplankton biomass exhibit a higher dimensionality in high hydrodynamic conditions, we cannot conclude, on the basis of the three previously used analysis techniques, to the existence of low-order deterministic chaos, but only to a lower dimensionality in low hydrodynamic conditions. The differential multifractal structures (Table 3) exhibited by temperature, salinity and phytoplankton biomass time series confirm and generalize the results suggested by the analysis techniques devoted to the identification of deterministic chaos.

5.1.3. Stochastic characterization of turbulent processes

The multifractal analysis techniques used in this paper have widely been shown to provide valid estimates of the whole stochastic behaviour of a given time series or transect, even when performed on small data sets, i.e., less than 1000 data points [30–32,65,84,85]. The multifractal parameters estimated for temperature, salinity and phytoplankton biomass in this study (Table 3) then clearly appear to be in the range of values previously obtained for a wide variety of tidal conditions in the Southern Bight of the North Sea, the Eastern English Channel and the St Lawrence estuary [27,30–32,34,44]. This shows that similar processes could be at the origin of both physical (i.e., temperature and salinity) and biological (phytoplankton biomass) temporal structure, and consequently that small-scale phytoplankton biomass distribution can be regarded as being passively advected by turbulent fluid motions, at least at the scale of the whole tidal cycle. However, correlation analyses have shown that temperature and salinity multifractal structures remain the same whatever the tidal conditions, while phytoplankton biomass exhibits very specific temporal patterns (Table 4). This then indicates that even in highly turbulent environments as the one experienced in the Eastern English Channel, phytoplankton biomass cannot be regarded as being a purely passive scalar even on smaller scales, but rather exhibit an altogether level of small-scale temporal structure related to the space–time scales of the tidal forcing. In particular, the observed significant negative correlation between multifractal structure of phytoplankton biomass and current speed indicate that the phytoplankton assemblages sampled in the present study are more heterogeneously distributed (i.e., high H and C_1, values) in low hydrodynamic conditions. Moreover, the values of the third multifractal parameter α ($\alpha = 1.82 \pm 0.06$ SD; Table 3) indicates that phytoplankton biomass cannot be regarded as log-normally distributed—in which case $\alpha = 2$—even in high hydrodynamic conditions. On the contrary, this value is typically in the range of α values estimated for phytoplankton biomass distribution over similar ranges of scales [27,30–32,34,44]. The positive correlation between α and the current speed nevertheless indicates a differential phytoplankton biomass structure characterized by a greater complexity in the hierarchy of its variability levels in high hydrodynamic conditions.

On the other hand, multifractal parameters (i.e., H and C_1; Table 4) are significantly correlated to current direction, but do not exhibit any significant correlation with mean phytoplankton biomass. This suggests that phytoplankton biomass structure cannot be regarded as resulting from any density-dependent process associated with tidal advection, but rather from the qualitative nature of phytoplankton assemblages occurring during ebb and flood, as previously suggested [32,34]. While many phenomenological hypotheses could be proposed to explain these differential temporal distributions of phytoplankton biomass—such as the differential effects of turbulence and phytoplankton composition on the formation, maintenance and structure of phytoplankton aggregates [86–90]—the resolution of this particular issue is beyond the scope of this contribution. One can nevertheless refer to Refs. [32,34] for further comments on the potential causes and consequences of small-scale heterogeneous phytoplankton distributions.

The universal multifractal formalism can also be related to the dimension formalism developed to study strange attractors. Especially, one may write [91]

$$v = d - K(2)\,, \tag{10}$$

where v is the correlation dimension defined above (see Eq. (9)), d is the Euclidean dimension of the observation space ($d = 1$ for time series, therefore the corresponding v estimate is for embedding dimension $E = 2$) and $K(2)$ is the second order scaling moment $K(q)$ defined as [60,61,92–94]:

$$K(q) = \frac{C_1}{\alpha - 1}(q^{\alpha} - q)\,, \tag{11}$$

where $K(q)$ is the scaling moment function which describes the multiscaling of the statistical moments of order q. Correlation dimensions v estimated from the correlation integral algorithm [see Eq. (9)] and from Eq. (10) where $K(2)$ is reached with C_1, α (Table 3) and $q = 2$ in Eq. (11) are then very similar for temperature, salinity and in vivo fluorescence (Fig. 8). The dimension formalism having been developed to describe attractors exhibiting a very high dimensionality, this result then confirms that the time series studied in the present paper are rather characterized by their high-order stochasticity rather than by any kind of low-order behaviour.

Nonlinear dynamical systems being capable of such a variety of behaviours, the present results indicate that the use of a single technique of time series analysis should not be relied on too heavily [95]. In particular, the emphasis of this paper is on supplementing techniques, rather than competing with them. When only one technique is used to analyze a time series, the results are expected to be at best incomplete, and at worst misleading. For instance, the infinite number of dimensions characterizing strange attractors [54,96,97] when specific mathematical tests (such as the correlation integral algorithm) fail to find any signs of low-order deterministic behaviour could be advantageously described in the framework of universal multifractals, i.e., high-order stochastic behaviour.

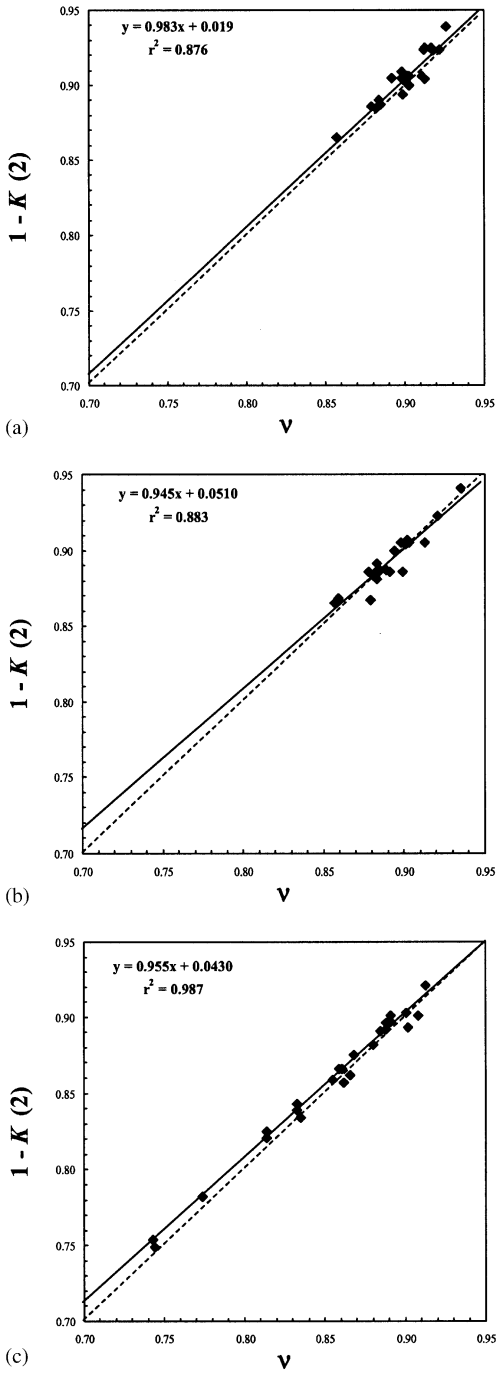

Fig. 8. Plots of the correlation dimension ν estimated following Eqs. (9) and (10), shown together with their best linear fit for temperature (a), salinity (b) and in vivo fluorescence (c) from the original 172,800 data points time series. The first bissectrix (dotted line) is shown for comparison.

5.2. Dealing with determinism and stochasticity: a challenge for future modelling in marine ecology

Following the great deal of attention recently devoted to detect and analyze chaos in plankton ecology [9,21–25], the results concerning the multifractal (i.e., stochastic) structure of plankton populations [26,30–34], and more generally the increasing amount of literature providing evidence for nonlinearity in population growth and ecological interactions [98–100] distinguishing between low dimensional deterministic chaos and high dimensional stochasticity then seems to be at the core of an emerging ecological thought process. Thus, as previously emphasized [14], 'the study of chaos is important for ecology because the lessons of nonlinear dynamics will provide very different answers than the linear models traditionally emphasized by ecologists'.

As developed above, the central tenet of deterministic chaos and stochasticity lies in their related predictive ability. Chaotic systems are predictable over short time scales because they are deterministic; the lack of predictive power over long-time scales stems from the lack of complete information about the exact location of initial conditions. In contrast, systems that are stochastic are unpredictable over any time scale because of the probabilistic nature of their components. Nevertheless, systems can have endogenous dynamics that are chaotic in the presence of exogenous stochastic perturbation. Such interactions between systems with chaotic dynamics and stochasticity leads to interesting behaviours [101–103]. The number of investigations of chaos in modelling ecological systems with stochasticity has nevertheless still been quite small. Thus, investigations of a logistic model with additive noise showed that chaotic dynamics persisted [102,104]. Rand and Wilson [103] emphasized how the interaction between the deterministic dynamics and noise can lead to a case where the average Lyapunov exponent is positive, even though the purely deterministic system with the same parameters is not chaotic. While these works provide further evidence for the ubiquity of chaos by showing that individual-based models can appear deterministic and chaotic at the level of the population, actual key challenges in the study of ecological systems involve ways to deal with the collective dynamics of various ensembles of individuals, and to understand how to relate phenomena across scales [105]. While Denman and Powell [106] emphasized that ecological responses could not be linked to a particular physical scale, transfers of variability across scales have indeed been found in models for predator-prey interactions that can display variability at frequencies other than that of the periodic (i.e., seasonal) forcing [7,107–109]. A direction of future research could then be to focus on the responses to more realistic stochastic forcing (i.e., multifractal) of such modelling approaches in terms of determinism and/or stochasticity.

Distinguishing between chaos and stochastic processes could also have considerable implications for the design and evaluation of sampling schemes in the coastal ocean. We indeed demonstrated here that the degree of stochasticity and/or determinism exhibited by phytoplankton populations varies with both hydrodynamical and advective conditions. It has also been demonstrated over a wider range of scales (i.e., from 1 s to 48 h) that the stochastic structure of phytoplankton biomass varies with the sampling scale [30–32]. In that way, Rand and Wilson [110] theoretically demonstrated that the optimal scale at which to measure a given process is described as the one that

'maximizes the ratio of deterministic information to stochastic fluctuations', while Pascual and Levin [111] developed a determinism test from nonlinear data analysis to describe and to identify a characteristic length scale at which to average spatio-temporal systems. Finally, one may note here that like most oceanographic data, the data analyzed here contain both spatial and temporal components, because sampling has been accomplished in the Eulerian sense, that is, in a reference frame fixed with respect to the moving fluid. While Seuront et al. [31] demonstrated that the stochastic structure of a given signal is wholly dependent on the scale of the sampling (i.e., Eulerian/Lagrangian transition), Eulerian sampling of spatially heterogeneous populations have also been suggested to obscure any deterministic signal beyond the resolving capabilities of presently available nonlinear signal processing techniques [15]. Thus, as previously suggested in a more general ecological framework [112,113], the grain and extent of a given sampling experiment, as the way the samples are taken, should be regarded as being essential components to the understanding of a given time series, as precise numerical values of Lyapunov exponents, correlations dimensions and multifractals parameters might be.

Thus, in the general background of spatio-temporal intermittency encountered in the ocean [38], future studies investigating the magnitude of keys fluxes such as primary production should take a great advantage to focus on the deterministic/stochastic duality to reach robust estimates and modelling of stocks and fluxes, all the more since numerical modelling are extremely sensitive even to minor changes in parameter values [114,115].

Acknowledgements

The author thanks Drs. F. Schmitt and C. Nicolis who offered constructive comments which greatly improved the manuscript. I also thank the captain and the crew of the N/O 'Côte de la Manche' for their assistance during the sampling experiment. This is a contribution of the Ecosystem Complexity Research Group (ECOREG).

References

[1] R.M. May, Biological populations with non-overlapping generations: stable points, stable cycles and chaos, Science 186 (1974) 645–647.
[2] R.M. May, Biological populations obeying difference equations: stable points, stable cycles and chaos, J. Theor. Biol. 51 (1975) 511–524.
[3] R.M. May, Simple mathematical models with very complicated dynamics, Nature 261 (1976) 459–467.
[4] M.P. Hassell, J.H. Lawton, R.M. May, Patterns of dynamical behaviour in single species population models, J. Anim. Ecol. 45 (1976) 471–486.
[5] A. Berryman, J. Milstein, Are ecological systems chaotic—and if not, why not? Trends Ecol. Evol. 4 (1989) 26–28.
[6] R. Pool, Is it chaos or is it just a noise? Science 243 (1989) 310–313.
[7] M. Kot, G.S. Sayler, T.W. Schultz, Complex dynamics in a model of microbial system, Bull. Math. Biol. 54 (1992) 619–648.
[8] A. Hastings, T.M. Powell, Chaos in a three species food chain, Ecology 72 (1991) 896–903.

[9] E.E. Popova, M.J.R. Fasham, A.V. Osipov, V.A. Ryabchenko, Chaotic behavior of an ocean ecosystem model under seasonal external forcing, J. Plankton Res. 19 (1997) 1495–1515.
[10] R.M. May, Nonlinear phenomena in ecology and epidemiology, Ann. N. Y. Acad. Sci. 357 (1980) 267–281.
[11] R.M. May, Chaos and the dynamics of biological populations, Proc. Soc. London Ser. A 413 (1987) 27–44.
[12] H.C.J. Godfrey, S.P. Blythe, Complex dynamics in multispecied communities, Philos. Trans. Roy. Soc. Ser. B 330 (1991) 221–233.
[13] S. Ellner, Detecting low dimensional chaos in population dynamic data: a critical review, in: J. Logan, F. Hain (Eds.), Chaos and Insect Ecology, University Press of Virginia, Blacksburg, 1992, pp. 63–91.
[14] A. Hastings, C.L. Hom, S. Ellner, P. Turchin, H.C.J. Godfray, Chaos in ecology: is mother nature a strange attractor?, Annu. Rev. Ecol. Syst. 24 (1993) 1–33.
[15] S. Ellner, P. Turchin, Chaos in a noisy world: new methods and evidence from time series analysis, Am. Nat. 145 (1995) 343–375.
[16] J.D. Farmer, J.J. Sidorowich, Predicting chaotic time series, Phys. Rev. Lett. 59 (1987) 845–848.
[17] J. Theiler, S. Eubank, A. Longtin, B. Galdrikian, J.D. Farmer, Testing for nonlinearity in time series: the method of surrogate data, Physica D 58 (1992) 77–94.
[18] D.M. Rubin, Use of forecasting signatures to help distinguishing periodicity, randomness and chaos in ripples and other spatial patterns, Chaos 2 (1992) 525–535.
[19] D.A. Rand, Measuring and characterizing spatial patterns, dynamics and chaos in spatially extended dynamical systems and ecologies, Philos. Trans. Roy. Soc. London Ser. A 348 (1994) 497–514.
[20] R.V. Solé, J. Bascompte, Measuring chaos from spatial informations, J. Theor. Biol. 175 (1995) 139–147.
[21] G. Sugihara, R.M. May, Nonlinear forecasting as a way of distinguishing chaos from measurement error in time series, Nature 344 (1990) 734–741.
[22] M. Scheffer, Should we expect strange attractors behind plankton dynamics—and if so, should we bother? J. Plankton Res. 13 (1991) 1291–1305.
[23] F.A. Ascioti, E. Beltrami, T.O. Carrol, C. Wirrick, Is there chaos in plankton dynamics? J. Plankton Res. 15 (1993) 603–617.
[24] P.G. Strutton, J.G. Mitchell, J.S. Parslow, Nonlinear analysis of chlorophyll a transects as a method of quantifying spatil structure, J. Plankton Res. 18 (1996) 1717–1726.
[25] P.G. Strutton, J.G. Mitchell, J.S. Parslow, Using nonlinear analysis to compare the spatial structure of chlorophyll with passive tracers, J. Plankton Res. 19 (1997) 1553–1564.
[26] M. Pascual, F.A. Asciotti, H. Caswell, Intermittency in the plankton: a multifractal analysis of zooplankton biomass variability, J. Plankton Res. 17 (1995) 1209–1232.
[27] S. Lovejoy, W.J.S. Currie, Y. Tessier, M.R. Claereboudt, E. Bourget, J.C. Roff, D. Schertzer, Universal multifractals and ocean patchiness: phytoplankton, physical fields and coastal heterogeneity, J. Plankton Res. 23 (2001) 117–141.
[28] L. Seuront, Fractals and multifractals: new tools to characterize space–time heterogeneity in marine ecology, Océanis 24 (1999) 123–158.
[29] L. Seuront, Y. Lagadeuc, Multiscale patchiness of the calanoid copepod Temora longicornis in a turbulent coastal sea, J. Plankton Res. 23 (2001) 1137–1145.
[30] L. Seuront, F. Schmitt, Y. Lagadeuc, D. Schertzer, S. Lovejoy, S. Frontier, Multifractal analysis of phytoplankton biomass and temperature in the ocean, Geophys. Res. Lett. 23 (1996) 3591–3594.
[31] L. Seuront, F. Schmitt, Y. Lagadeuc, D. Schertzer, S. Lovejoy, Multifractal intermittency of Eulerian and Lagrangian turbulence of ocean temperature and plankton fields, Nonlin. Proc. Geophys. 3 (1996) 236–246.
[32] L. Seuront, F. Schmitt, Y. Lagadeuc, D. Schertzer, S. Lovejoy, Universal multifractal analysis as a tool to characterise multiscale intermittent patterns. Example of phytoplankton distribution in turbulent coastal waters, J. Plankton Res. 21 (1999) 877–922.
[33] L. Seuront, F. Schmitt, Y. Lagadeuc, Turbulence intermittency, small-scale phytoplankton patchiness and encounter rates in plankton: where do we go from here?, Deep-Sea Research I 48 (2001) 1199–1215.

[34] L. Seuront, V. Gentilhomme, Y. Lagadeuc, Small-scale nutrient patches in tidally mixed coastal waters, Mar. Ecol. Prog. Ser. 232 (2002) 29–44.
[35] B. Mandelbrot, The Fractal Geometry of Nature, Freeman, New York, 1983.
[36] M.A. Baker, C.H. Gibson, Sampling turbulence in the stratified ocean: statistical consequences of strong intermittency, J. Phys. Oceanogr. 17 (1987) 1817–1836.
[37] H.O. Peitgen, H. Jurgens, D. Saupe, Chaos and Fractals: News Frontiers of Science, Springer, New York, 1992.
[38] T. Platt, W.G. Harrison, M.R. Lewis, W.K.W. Li, S. Sathyendranath, R.E. Smith, A.F. Vezina, Biological production of the oceans: the case for a consensus, Mar. Ecol. Prog. Ser. 52 (1989) 77–88.
[39] M. Bohle-Carbonell, Sampling turbulence in the stratified ocean: statistical consequences of strong intermittency, Cont. Shelf Res. 12 (1992) 3–24.
[40] D. Ruelle, F. Takens, On the nature of turbulence, Comm. Math. Phys. 20 (1971) 167–192.
[41] D. Schertzer, S. Lovejoy, The dimension and intermittency of atmospheric dynamics, in: B. Launder (Ed.), Turbulent Shear Flows 4, Springer, Karlsruhe, 1983, pp. 7–33.
[42] G. Parisi, U. Frisch, A multifractal model of intermittency, in: M. Ghil, R. Benzi, G. Parisi (Eds.), Turbulence and Predictability in Geophysical Fluid Dynamics and Climate Dynamics, North-Holland, Amsterdam, 1985.
[43] R. Benzi, G. Paladin, G. Parisi, G. Vulpiani, On the multifractal nature of fully developed turbulence and chaotic systems, J. Phys. A 17 (1984) 3521–3531.
[44] L. Seuront, Space-time heterogeneity and bio-physical coupling in pelagic ecologie: implications on carbon fluxes estimates, Ph.D. Thesis, Université des Sciences et Technologies de Lille, France, 1999.
[45] J.M. Brylinski, Y. Lagadeuc, V. Gentilhomme, J.P. Dupont, R. Lafite, P.A. Dupeuple, M.F. Huault, Y. Auger, E. Puskaric, M. Wartel, L. Cabioch, Le 'fleuve côtier': un phénomène hydrologique important en Manche orientale: exemple du Pas-de-Calais, Oceanol, Acta 11 (1991) 197–203.
[46] J.M. Brylinski, D. Bentley, C. Quisthoudt, Discontinuité écologique et zooplancton (copépodes) en Manche orientale, J. Plankton Res. 10 (1984) 503–513.
[47] J.M. Brylinski, Y. Lagadeuc, L'interface eau côtière/eau du large dans le Pas-de-Calais (côte française: une zone frontale, C. R. Acad. Sci. Paris. Sér. 2 311 (1990) 535–540.
[48] Y. Lagadeuc, J.M. Brylisnki, D. Aelbrecht, Temporal variability of the vertical stratification of a front in a tidal region of freshwater influence (ROFI) system, J. Mar. Syst. 12 (1997) 147–155.
[49] P. Legendre, L. Legendre, Numerical Ecology, Elsevier, Amsterdam, 2003.
[50] R.R. Sokal, F.J. Rohlf, Biometry, The Principles and Practice of Statistics in Biological Research, Freeman, San Francisco, 1995.
[51] N.H. Packard, J.P. Crutchfield, J.D. Farmer, R.S. Shaw, Geometry from a time series, Phys. Rev. Lett. 45 (1980) 712–716.
[52] F. Takens, Detecting strange attractors in turbulence, Lect. Notes Math. 898 (1981) 366–381.
[53] A. Wolf, J.B. Swift, H.L. Swinney, J.A. Vastano, Determining Lyapunov exponents from a time series, Physica D 16 (1985) 285–317.
[54] I. Grassberger, I. Procaccia, Characterization of strange attractors, Phys. Rev. Lett. 50 (1983) 346–349.
[55] A.A. Tsonis, J.B. Elsner, K.P. Georgakakos, Estimating the dimension of weather and climate attractors: important issues about the procedure and interpretation, J. Atmos. Sci. 50 (1993) 2549–2555.
[56] E.N. Lorenz, Deterministic nonperiodic flow, J. Atmos. Sci. 20 (1963) 130–141.
[57] M.D. Mundt, W.B. Maguire, R.R.P. Chase, Chaos in the sunspot cycle: analysis and prediction, J. Geophys. Res. 96 (1991) 1705–1716.
[58] J. Feder, Fractal, Plenum, New York, 1988.
[59] U. Frisch, Turbulence: The Legacy of A.N. Kolmogorov, Cambridge University Press, New York, 1995.
[60] D. Schertzer, S. Lovejoy, Physically based rain and cloud modeling by anisotropic multiplicative turbulent cascades, J. Geophys. Res. 92 (1987) 9693–9714.
[61] D. Schertzer, S. Lovejoy, Nonlinear variability in geophysics: multifractal analysis and simulation, in: L. Pietronero (Ed.), Fractals: Physical Origin and Consequences, Plenum, New York, 1989, pp. 49–79.

[62] F. Schmitt, S. Lovejoy, D. Schertzer, Multifractal analysis of the Greenland ice-core project climate data, Geophys. Res. Lett. 22 (1995) 1392–1689.
[63] F. Schmitt, D. Schertzer, S. Lovejoy, Y. Brunet, Multifractal temperature and flux of temperature in fully developed turbulence, Europhys. Lett. 34 (1996) 195–200.
[64] F. Schmitt, D. Schertzer, S. Lovejoy, Y. Brunet, Multifractal properties of temperature fluctuations in turbulence, in: M. Giona, G. Biardi (Eds.), Fractals and Chaos in Chemical Engineering, World Scientific, Singapore, 1996, pp. 464–475.
[65] F. Schmitt, D. Schertzer, S. Lovejoy, Multifractal modeling of turbulent fluctuations in finance, in: F. Marsella, G. Salvadori (Eds.), Chaos, Fractals and Models, Italian University Press di Giovanni Iuculano, Pavia, 1998, pp. 150–157.
[66] D. Lavallée, S. Lovejoy, D. Schertzer, F. Schmitt, On the determination of universal multifractal parameters in turbulence, in: K. Moffat, M. Tabor, G. Zaslavsky (Eds.), Topological Aspects of the Dynamics of Fluid and Plasmas, Kluwer, Boston, 1992, pp. 463–478.
[67] F. Schmitt, D. Lavallée, D. Schertzer, S. Lovejoy, Empirical determination of universal multifractal exponents in turbulent velocity fields, Phys. Rev. Lett. 68 (1992) 305–308.
[68] F. Schmitt, D. Schertzer, S. Lovejoy, Y. Brunet, Estimation of universal multifractal indices for atmospheric turbulent velocity fields, Fractals 1 (1993) 568–575.
[69] F. Schmitt, D. Schertzer, S. Lovejoy, Y. Brunet, Empirical study of multifractal phase transitions in atmospheric turbulence, Nonlin. Proc. Geophys. 1 (1994) 95–104.
[70] D. Schertzer, S. Lovejoy, Generalised scale invariance in turbulent phenomena, Physico-Chem. Hydrodyn. J. 6 (1985) 623–635.
[71] A. Kawamura, M. Matsumoto, K. Jinno, S. Xu, Estimation and prediction for dynamics of chaotic time series (I). On the dependence of Lorenz equation on the initial value and parameters and its prediction by nonlinear least square method, Technology Reports of Kyushu University 67 (1994) 513–521.
[72] A. Kawamura, M. Matsumoto, K. Jinno, S. Xu, Estimation and prediction for dynamics of chaotic time series (II). On the estimation and prediction for dynamics of Lorenz equation by extended Kalman filter, Technol. Rep. Kyushu Univ. 67 (1994) 523–531.
[73] S. Ellner, A.R. Gallant, D. McCaffrey, D. Nychka, Convergence rates and data requirements for Jacobian-based estimates of Lyapunov exponents from data, Phys. Lett. 153 (1991) 357–363.
[74] D. Nychka, S. Ellner, A.R. Gallant, D. McCaffrey, Finding chaos in noisy systems, J. Royal Stat. Soc. B 54 (1992) 399–426.
[75] I. Rodriguez-Iturbe, B.F. de Power, M.B. Sharifi, K.B. Georgakakos, Chaos in rainfall, Wat. Resour. Res. 25 (1989) 1667–1675.
[76] J.B. Ramsey, H.J. Yuan, Bias and error bars in dimension calculations and their evaluations in some simple models, Phys. Lett. A 134 (1989) 287–297.
[77] J.C. Vassilicos, A. Demos, F. Tata, No evidence of chaos but some evidence of multifractals in the foreign exchange and stock markets, in: A.J. Crilly, R.A. Eranshaw, H. Jones (Eds.), Applications of Fractals and Chaos, The Shape of Things, Springer, Berlin, 1993, pp. 249–265.
[78] G.D. Jeong, A.R. Rao, Chaos characteristics of tree ring series, J. Hydrol. 182 (1996) 239–257.
[79] S. Kauffman, The Origins of Order, Oxford University Press, New York, 1993.
[80] S. Kauffman, S. Johnsen, Coevolution to the edge of chaos: coupled fitness landscapes, poised states, and coevolutionary avalanches, J. Theor. Biol. 149 (1991) 467–505.
[81] C.G. Langdon, Life at the edge of chaos, in: C.G. Langdon, C. Taylor, J.D. Farmer, S. Rasmussen (Eds.), Artificial Life II, Addison-Wesley, Redwood City, 1992, pp. 41–91.
[82] L.A. Smith, Intrinsic limits on dimension calculations, Phys. Lett. A 133 (1988) 283–288.
[83] F. Ibanez, Le déterminisme du chaos, J. Rech. Océanogr. 11 (1986) 66–69.
[84] Y. Teissier, S. Lovejoy, D. Schertzer, Universal multifractals: theory and observations of rain and clouds, J. Appl. Meteor. 32 (1993) 223–250.
[85] Y. Tessier, S. Lovejoy, D. Schertzer, D. Lavallée, B. Kerman, Universal multifractal indices for the ocean surface at far red wavelength, Geophys. Res. Lett. 20 (1993) 1167–1170.
[86] U. Riebesel, Particle aggregation during a diatom bloom, I. Physical aspects, Mar. Ecol. Prog. Ser. 69 (1991) 273–280.

[87] U. Riebesel, Particle aggregation during a diatom bloom, II. Biological aspects, Mar. Ecol. Prog. Ser. 69 (1991) 281–291.
[88] T. Kiørboe, Small-scale turbulence, marine snow formation, and planktivorous feeding, Sci. Mar. 61 (1997) 141–158.
[89] T. Kiørboe, C. Lunsgaard, M. Olesen, J.L.L.S. Hansen, Aggregation and sedimentation processes during a spring phytoplankton bloom: a field experiment to test coagulation theory, J. Mar. Res. 52 (1994) 297–323.
[90] T. Kiørboe, P. Tiselius, B. Mitchell-Innes, J.L.S. Hansen, A.W. Wisser, X. Mari, Intensive aggregate formation with low vertical flux during an upwelling-induced diatom bloom, Limnol. Oceanogr. 43 (1998) 104–116.
[91] T.C. Halsey, M.H. Jensen, L.P. Kadanoff, I. Procaccia, B.I. Shraiman, Fractal measures and their singularities: the characterization of strange sets, Phys. Rev. A 33 (1986) 443–453.
[92] D. Schertzer, S. Lovejoy, Universal multifractals do exist!, J. Appl. Meteorol. 36 (1997) 1296–1303.
[93] D. Schertzer, S. Lovejoy, D. Lavallee, F. Schmitt, Universal hard multifractal turbulence, theory and observations, in: R.Z. Sagdeev, U. Frisch, F. Hussain, S.S. Moiseev, N.S. Erokhin (Eds.), Nonlinear Dynamics of Structures, World Scientific, Singapore, 1991, pp. 213–235.
[94] S. Lovejoy, D. Schertzer, Multifractals, universality classes and satellite and radar measurements of cloud and rain fields, J. Geophys. Res. 95 (1990) 2021–2034.
[95] M. Casdagli, Chaos and deterministic versus stochastic nonlinear modelling, J. R. Statist. Soc. B 54 (1991) 303–328.
[96] I. Grassberger, Generalized dimensions of strange attractors, Phys. Lett. A 97 (1983) 227–230.
[97] H.G.E. Hentschel, I. Procaccia, The infinite number of generalized dimensions of fractals and strange attractors, Physica D 8 (1983) 435–444.
[98] O.N. Björnstad, M. Begon, N.C. Stenseth, W. Falck, S.M. Sait, D.J. Thompson, Population dynamics of the Indian meal moth: demographic stochasticity and delayed regulatory mechanisms, J. Anim. Ecol. 67 (1998) 110–126.
[99] B.T. Grenfell, K. Wilson, B.F. Finkenstadt, T.N. Coulson, S. Murray, S.D. Albon, J.M. Pemberton, T.H. Clutton-Brock, M.J. Crawley, Noise and determinism in synchronized sheep dynamics, Nature 394 (1998) 674–677.
[100] N.C. Stenseth, K.S. Chan, E. Framstad, H. Tong, Phase- and density-dependent dynamics in Norwegian lemmings: interaction between deterministic and stochastic processes, Proc. Roy. Soc. London Ser. B 265 (1998) 1957–1968.
[101] J.P. Crutchfield, J.D. Farmer, B.A. Huberman, Fluctuations and simple chaotic dynamics, Phys. Rep. 92 (1982) 45–82.
[102] A. Rabinovitch, R. Thieberger, Biological populations obeying a stochastically perturbed logistic difference equation, J. Theor. Biol. 131 (1988) 509–514.
[103] D.A. Rand, H.B. Wilson, Chaotic stochasticity: a ubiquitous source of unpredictability in epidemics, Proc. Roy. Soc. London Ser. B 246 (1991) 179–184.
[104] W.M. Schaffer, S. Ellner, M. Kot, Effects of noise on some dynamical models in ecology, J. Math. Biol. 24 (1986) 479–523.
[105] S.A. Levin, B. Grenfell, A. Hastings, A.S. Perelson, Mathematical and computational challenges in population biology and ecosystems science, Science 275 (1997) 334–343.
[106] K.L. Denman, T.M. Powell, Effects of physical processes on planktonic ecosystems in the coastal ocean, Oceanogr. Mar. Biol. Ann. Rev. 22 (1984) 125–168.
[107] S. Rinaldi, S. Muratori, Y. Kuznetzov, Multiple attractors, catastrophes, and chaos in seasonally perturbed predator-prey communities, Bull. Math. Biol. 55 (1993) 15–36.
[108] M. Pascual, H. Caswell, H. From the cell-cycle to population cycles in phytoplankton-nutrient interactions, Ecology 78 (1997) 897–912.
[109] M. Pascual, H. Caswell, Environmental heterogeneity and biological pattern in a chaotic predator-prey system, J. Theor. Biol. 185 (1997) 1–13.
[110] D.A. Rand, H.B. Wilson, Using spatio-temporal chaos and intermediate-scale determinism to quantify spatially extended ecosystems, Proc. Roy. Soc. London Ser. B 259 (1995) 111–117.
[111] M. Pascual, S.A. Levin, From individuals to population densities: searching for the intermediate scale of nontrivial determinism, Ecology (1999).

[112] J.A. Wiens, Spatial scaling in ecology, Funct. Ecol. 3 (1989) 385–397.
[113] P.G. Jarvis, Scaling processes and problems, Plant, Cell and Environment 18 (1995) 1079–1089.
[114] F.E. Werner, F.H. Page, D.R. Lynch, J.W. Loder, R.G. Lough, R.I. Perry, D.A. Greenberg, M.M. Sinclair, Influences of mean advection and simple behavior on the distribution of cod and haddock early life stages on Georges Bank Fish, Oceanogr. 2 (1993) 43–64.
[115] E.A. Fulton, A.D.M. Smith, C.R. Johnson, Effect of complexity on marine ecosystem models, Mar. Ecol. Prog. Ser. 253 (2003) 1–16.